RJC

RASĀYAN *J. Chem.*
Vol. 18 | No. 4 |1999-2005| October-December | 2025
ISSN: 0974-1496 | e-ISSN: 0976-0083 | CODEN: RJCABP
http://www.rasayanjournal.com
http://www.rasayanjournal.co.in

ISOLATION, CHARACTERIZATION, AND COMPUTATIONAL DOCKING ANALYSIS OF CELLULOSE NANOCRYSTALS FROM *Morinda citrifolia* (NONI) LEAF FIBERS

Alphy J. Maliackal and Britto S.✉
Department of Chemistry, St Joseph's College (Autonomous), Affiliated to Bharathidasan University, Tiruchirappalli- 620002, Tamil Nadu, India
✉Corresponding author: britto_ch1@mail.sjctni.edu

ABSTRACT

Cellulose nanocrystals (CNCs) derived from *Morinda citrifolia* (noni) leaf fibers were explored as sustainable, biodegradable reinforcement agents in organic–inorganic nanocomposites, with a focus on catalytic applications. This study investigates the suitability of noni leaf fibers as a sustainable source for cellulose nanocrystal production (CNCs). The fibers underwent a sequential treatment process involving dewaxing, alkaline delignification, $KMnO_4$–oxalic acid bleaching, and acid hydrolysis. Each stage of the process was systematically characterized. Morphological analysis via scanning electron microscopy (SEM) revealed structural transformations, while Fourier transform infrared spectroscopy (FTIR) confirmed the progressive removal of non-cellulosic components. XRD analysis showed increased crystallinity with successive treatments, and thermo-gravimetric analysis (TGA) of CNC represented the weight loss in the sample, after being continuously heated to 600°C. Molecular docking studies using the breast cancer-related protein (3EQM) indicated a strong binding affinity of CNCs to the active site, with a binding energy of −8.5 kcal/mol, supported by hydrogen bond interactions, highlighting their potential for biomedical and drug delivery applications.

Keywords: Noni Leaf Fibers, Biomass Resource, Cellulose Nanocrystals, Nanocomposites, Molecular Docking.
RASĀYAN *J. Chem.*, Vol. 18, No. 4, 2025

INTRODUCTION

In recent years, natural fibers have gained significant attention as reinforcement fillers in composite materials due to their wide-ranging industrial applications, including pharmaceuticals, polymers, paper, catalysis, energy, electronics, and environmental sectors.[1] Their advantages include low density, high flexibility, biodegradability, cost-effectiveness, renewability, and wide availability. Natural fibers primarily consist of cellulose of hydrophilic behavior, made of poly units of (1,4-β-D-anhydroglucopyranose). Hemicelluloses and lignin constitute another principal component of plant fibers, with amorphous in nature. Cellulose consists of crystalline and amorphous regions, with the former being isolated as cellulose nanocrystals (CNCs) via acid hydrolysis. This selective removal enhances crystallinity and improves structural, surface, and thermal properties.[3] Cellulose nanocrystals (CNCs), commonly referred to as nano whiskers, are stiff, rod or sphere-shaped particles with superior properties such as biocompatibility, renewability, optical transparency, and biodegradability[1]. They can be derived from diverse sources like wood pulp, algae, and agro-industrial biomass, including rice straw[5], pineapple leaves[6], rice husk[7], sugarcane bagasse, and bamboo.[9] *Morinda citrifolia* (Noni), from the Rubiaceae family, is a potential new source of CNC due to its notable 31.29% cellulose alongside 25.01% hemicellulose, 18.34% lignin, 14.39% extractives, and 10.03% ash.[10] Though it is widely studied for its medicinal value, its fiber remains underexplored for CNC production. In this study, CNCs were extracted from Noni leaf fibers through a simple four-step process: dewaxing, alkaline treatment (NaOH), bleaching with $KMnO_4$–oxalic acid, and acid hydrolysis. The $KMnO_4$–oxalic acid system is an eco-friendlier bleaching agent that effectively removes lignin without degrading cellulose.[11] However, not much attention has been put forward on the isolation of cellulose from *M. citrifolia* fiber, and also the bleaching process using the $KMnO_4$-oxalic acid system is not well explored. The plant *M. citrifolia* is thoroughly investigated for its medicinal values, but very hardly consumed as the main CNC source. Here, we characterize the extracted CNCs using FTIR, SEM, TGA, and XRD to assess morphology, thermal stability, and crystallinity. Additionally, the potential

http://doi.org/10.31788/RJC.2025.1849426

of CNC in biomedical applications was evaluated via molecular docking against the breast cancer-associated protein (3EQM) using AutoDock Vina, demonstrating strong binding affinity and suggesting possible use in drug delivery systems.

EXPERIMENTAL

Material

The *Morinda citrifolia* fibers were collected from an agricultural field in Thodupuzha, Kerala, India. Sodium hydroxide pellets, n-hexane, ethyl alcohol, $KMnO_4$, Oxalic acid, and Sulphuric acid were procured from Merck, India, and they were used without any further purification.

General Procedure

Extraction of Cellulose and Nano-Cellulose

M. citrifolia fibers (MCF) were first cleaned, dried, and powdered. The raw materials were consecutively dewaxed through immersing and agitating them in n-hexane, followed by ethanol and distilled water washes. The dewaxed MCF was heated in 10%NaOH at 80°C for 3h. Alkali-treated MCF(AMCF) were washed repeatedly until a neutral pH was obtained and kept on further treatment with 5g/L $KMnO_4$ solution at pH 4 for 30 min at 90°C using to fiber-to-liquor ratio, 1:30 and washed with water. The $KMnO_4$-treated fiber was mixed with 10g/L oxalic acid at 85°C for 30 min for the removal of excess permanganate.[11] After the bleaching process, plant fibers were rinsed with water many times to keep a neutral pH. Following the bleaching treatments, the MCF became white, indicating the removal of lignin. To perform acid hydrolysis, 5 g of bleached *M. citrifolia* fibers (BMCFs) were mixed with 63% sulfuric acid at a 1:10 fiber-to-liquor ratio and stirred vigorously at 45 °C for 15 minutes. To terminate the acid hydrolysis, ice-cold water was added, and the mixture was left to equilibrate to room temperature before being centrifuged to isolate cellulose nanocrystals. Finally, the fibers were subsequently dispersed in deionized water (Fig.-1).

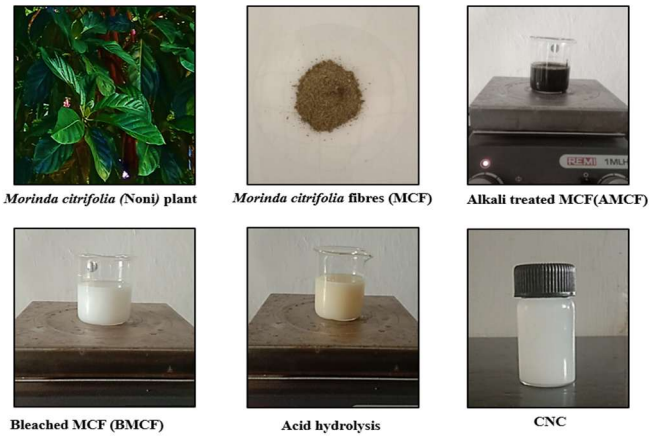

Fig.-1: Extraction Stages of Cellulose Nanocrystals (CNCs) from *Morinda citrifolia* Fibers (MCFs)

Characterization Methods

Characterization of the samples was carried out using various analytical techniques. FTIR spectroscopy (PerkinElmer Spectrum Two) was employed to monitor the progressive removal of non-cellulosic components from the fibers, with spectra recorded in the 4000–400 cm^{-1} range, revealing overlapping peaks from different functional groups. X-ray diffraction (XRD) investigation was performed using a PANALYTICAL X'PERT3 diffractometer (Cu Kα radiation, λ = 1.5406 Å; 40 kV, 30 mA) across a 2θ range of 10–80°. The crystallinity index (CI) was calculated using Segal's equation 12, where I_{200} (2θ = 22.2°) represents both crystalline and amorphous regions, and I_{am} (2θ = 18.7°) indicates amorphous content. Crystallite size was estimated using Scherrer's equation, incorporating constants such as the Scherrer factor (k = 0.91), wavelength (λ = 0.1540 nm), Bragg angle (θ), and FWHM (β). SEM imaging (Carl Zeiss EVO-18) was conducted at 10 kV to observe morphological changes in MCF, AMCF, BMCF, and CNC at different magnifications. Thermogravimetric analysis (TGA) was performed using a METTLER TOLEDO TGA 2 with STAR e software, where 3.89 mg of sample was heated from 30 to 600 °C at 10 K/min in a ceramic crucible under a nitrogen flow rate of 60 mL/min to assess thermal stability.

Molecular Docking Studies

The molecular docking of CNC with the breast cancer-associated protein aromatase cytochrome P450 (PDB ID: 3EQM) was performed using AutoDock Vina.[13] The protein structure was obtained from the RCSB PDB and prepared by removing co-crystallized ligands, solvents, and cofactors. Polar hydrogens and Kollman charges were added using AutoDock Tools. The CNC ligand was modeled in ChemDraw 12.0, converted to 3D, and prepared in pdbqt format with defined torsional flexibility. Docking was conducted using a rigid receptor and flexible ligand, with the grid box set to 40 × 40 × 40 Å (centered at 85.730 × 50.115 × 43.537, spacing 0.375 Å) to target the active site. The best pose was selected based on the lowest binding energy, and interactions were analyzed using Discovery Studio.

RESULTS AND DISCUSSION

Fourier Transform Infrared Spectroscopy (FT-IR)

FTIR analysis of untreated and chemically treated *Morinda citrifolia* fibers (Fig.-2) highlights changes in cellulose, hemicellulose, and lignin due to stepwise treatments.

Natural fibers contain oxygen-rich functional groups of alkanes, alcohols, ketones, esters, and aromatics from components like cellulose, hemicellulose, and lignin.[14-15] Each spectrum showed two main regions: 800-1800 cm^{-1} and 2700-3700 cm^{-1}.

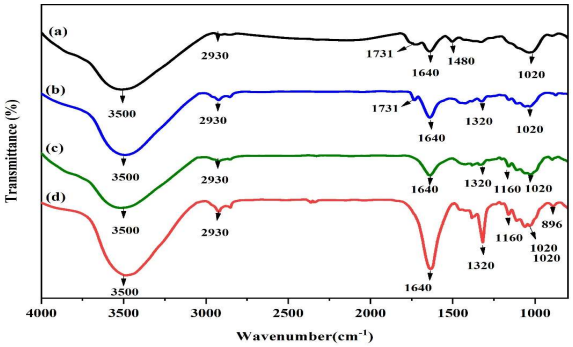

Fig.-2: FT-IR Spectra of (a). MCF (b). AMCF (c). BMCF (d). CNC

Broad peaks between 3000–3700 cm^{-1} correspond to –OH stretching of cellulose glucose units and moisture[16], while a band near 2930 cm^{-1} indicates C–H stretching vibrations of cellulose glucose units[17]. The sharp peak at 1640 cm^{-1} is linked to H_2O bending vibrations absorbed inside the cellulose fiber structure. The peak near 1480 cm^{-1} corresponds to C–C=C stretching in lignin, which decreases with NaOH treatment and disappears after bleaching, indicating effective lignin removal. The absence of the 1731 cm^{-1} hemicellulose peak in treated samples further confirms effective delignification and hemicellulose removal. A band at 1320 cm^{-1} reflects CH_2 twisting, while C–OH stretching and C–O–C glycosidic bond vibrations are reflected by the peaks at 1160 cm^{-1} and 1020 cm^{-1}, respectively. The peak observed at 1020 cm^{-1} in all spectra corresponds to the vibration of the C–O–C linkage in the pyranose ring, and the increased intensity of this band indicates enhanced crystallinity of the fibers after each chemical treatment. A characteristic band near 896 cm^{-1} confirms the presence of β-glycosidic linkages in the cellulose structure.[5] FTIR thus confirms the progressive removal of amorphous constituents and successful CNC formation, resulting in a stable, well-dispersed colloidal suspension.

XRD Analysis

The removal of amorphous lignin and hemicellulose during CNC extraction improves both crystallinity and crystallite size.[2] The crystallinity index (CI), defined as the ratio of crystalline to total diffraction intensity, was assessed using XRD. Figure-3 presents the XRD patterns of *M. citrifolia* fibers at various treatment stages, with CI values summarized in Table-1. Distinct peaks at 2θ = 15.9°, 22.5°, and 35° (Fig.-3a & b) confirm the cellulose I structure. Untreated fibers exhibited the lowest CI of 54.91%, attributed to their high amorphous content.

CI increased to 74.77% following alkali and bleaching treatments, with alkaline treatment showing a more significant impact. After acid hydrolysis, the CNC showed a CI of 83.27%, indicating a notable improvement in crystalline structure. Crystallite size, calculated using the Scherrer equation, was

approximately 4.04 nm. This rise in CI reflects the effective removal of waxes, hemicellulose, and lignin from raw Noni fiber.[18-19]

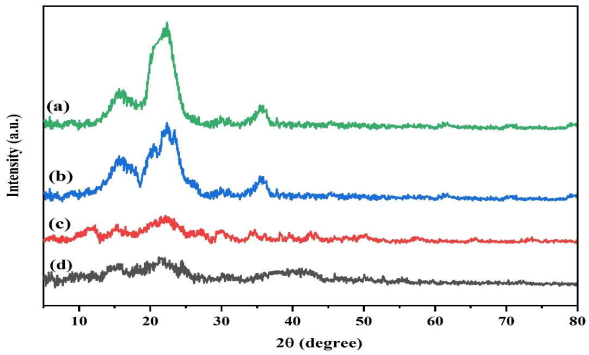

Fig.-3: XRD Profiles of (a) CNC, (b) BMCF, (c) AMCF, (d) MCF

Table-1: Crystallinity Index (CI) of (MCF) Measured at Various Stages of Chemical Treatment

Sample	2θ (Degree)	I_{am}	2θ (Degree)	I_{002}	CI (%)
MCF	18.7	37.17	21.5	82.44	54.91
Alkali-Treated MCF	18.4	28.74	22.1	87.12	67.01
Bleached MCF	18.4	25.14	22.1	99.68	74.77
CNC	18.7	60.45	22.3	361.54	83.27

Morphological Analysis

SEM analysis was used to observe the morphological changes in *M. citrifolia* leaf fibers throughout the extraction process, as shown in Fig.-4. The raw fiber (Fig.-4a) exhibits a smooth surface, indicating the presence of lignin, hemicellulose, waxes, and oils.[20] After alkali treatment (Fig.-4b), the fiber surface appears rough, suggesting partial removal of non-cellulosic components.[21] Bleaching further alters the fiber color to white, confirming significant lignin removal.[14] NaOH promotes the hydrolysis of ester and glycosidic bonds in hemicellulose, breaking it down into soluble sugars. Ether linkages and other chemical connections in the lignin structure dissociate because lignin is more soluble in alkaline solutions than in water. Because of this change, the lignin can degrade and get dissolved in an alkaline solution while separating from the fiber.[22] Finally, CNCs (Fig.-4d) display a cylindrical morphology with a high aspect ratio, indicating successful isolation of nanocellulose.

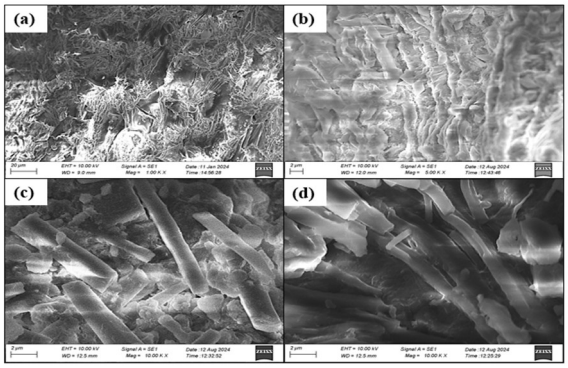

Fig.-4: SEM images of (a) MCF, (b) AMCF, (c) BMCF, and (d) CNC

Thermal Properties

Thermogravimetric–differential thermogravimetric (TG–DTG) analysis was performed on the CNC powder extracted from Noni fibers to evaluate its thermal degradation behavior. As shown in Fig.-5, the TG–DTG curves of CNC exhibit significant weight loss and associated peak degradation temperatures. The TG profile tracks thermal weight loss, whereas the DTG curve indicates the temperature at which degradation occurs most rapidly. The DTG curve (Fig.-5) shows a 9.27% mass loss at 53.1 °C, within 30–100 °C, caused by the evaporation of absorbed moisture. An inflection point was observed between 100–470 °C, a peak at 360.5 °C on the DTG curve corresponds to significant thermal degradation, resulting in

80.5% weight loss. The observed weight loss results from thermal degradation of cellulose at this heating temperature.[23] The residual mass remaining at 600 °C was 10.23%. A portion of this residual weight in the acid-hydrolysed cellulose is ascribed to the presence of lignin, which degrades slowly and therefore contributes to an elevated residual mass when present.[24] The unburned residue is likely due to ash content, which does not undergo thermal decomposition below the final temperature.

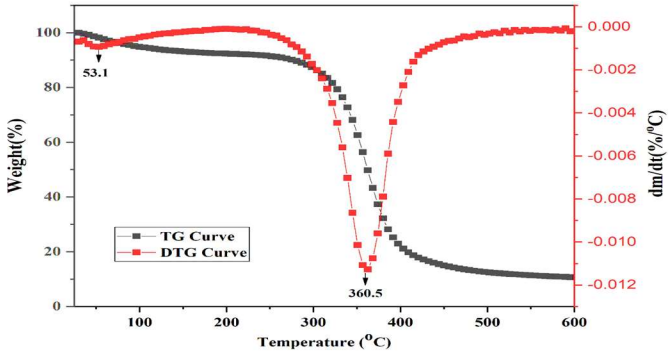

Fig.-5: Thermogravimetric (TG) and Differential Thermogravimetric (DTG) Curves of CNC from Noni Leaf Fibers

Docking Studies

Molecular docking of CNC with the breast cancer-related protein aromatase cytochrome P450 (PDB ID: 3EQM) was performed using AutoDock. CNC exhibited strong binding within the active site, with interaction energies ranging from –8.5 to –7.3 kcal/mol. Figure-6 displays a graphical depiction of the best docking pose with the CNC ligand and the 3EQM protein. Based on the docking outcomes indicate that the interactions between the target protein and ligand sites of the sample are mediated through both inter- and intramolecular hydrogen bonds, with bond lengths below 4 Å, confirming interaction stability.

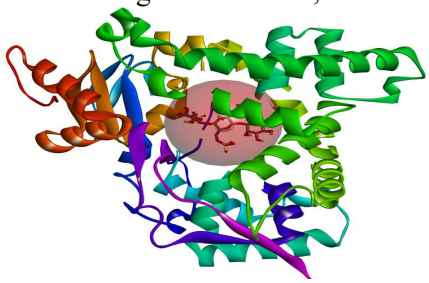

Fig.-6: Best Docked Pose between the 3EQM Protein and the CNC Ligand

Key residues involved include ARG375, ARG115, LEU372, THR310, and CYS437, forming hydrogen bonds at 2.69, 2.33, 2.41, 2.53, 3.61, and 3.54 Å, respectively (Fig.-7a & b). The inhibition constant (Ki), assessed using the equation $Ki = e^{(\Delta G/RT)}$, was approximately 0.588 µM, where ΔG represents the docking binding energy, T is the temperature (25 °C), and R the gas constant (1.9872036×10^{-3} kcal/mol K), suggesting a strong binding affinity of CNC to the target protein.[25]

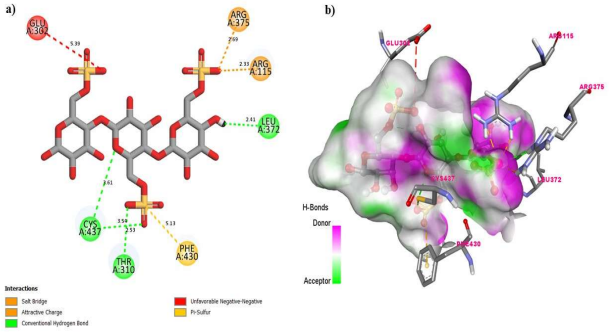

Fig.-7: (a) Two-dimensional Representation of Hydrogen Bond Interactions between the CNC Ligand and the 3EQM Protein, (b) Receptor-Side Surface Visualization of Hydrogen Bonding between the CNC Ligand and the 3EQM Protein

CONCLUSION

Cellulose nanocrystals (CNC) were efficaciously isolated from a renewable, abundant, and low-cost natural source, *Morinda citrifolia* (Noni) leaves, via the $KMnO_4$-Oxalic acid bleaching method followed by acid hydrolysis. The alkali process (NaOH) and $KMnO_4$-oxalic acid bleaching have effectively eliminated non-cellulosic components, yielding cellulose-rich fibers. The successful conversion of microcellulose into nanocellulose, achieving a crystallinity index of 83.27% and demonstrating remarkable thermal stability, has been confirmed through characterization methods including FTIR, XRD, SEM, and TGA/DTG. The derived CNC exhibited a cylindrical morphology with an average crystallite size is 4.04 nm. MCF-derived CNCs represent a novel and advantageous reinforcement agent in sustainable biopolymer nanocomposites for diverse applications, including water purification, bioplastics, biomedical devices, nano catalysts making, and eco-friendly engineering products. Additionally, molecular docking studies of CNC with human placental aromatase cytochrome P450 (3EQM) revealed consistent interactions between the ligand and active site residues, thereby validating the current docking protocols.

ACKNOWLEDGMENTS

The authors thank DST-FIST, Government of India, for funding towards infrastructure and instrumentation facilities at ACIC, St. Joseph's College (Autonomous), Tiruchirappalli, India. Both authors are grateful for the financial support from the management of St. Joseph's College, Tiruchirappalli, India, through SJCRG 2024-26 and 2025-26.

CONFLICT OF INTERESTS

The authors declare that there is no conflict of interest.

AUTHOR CONTRIBUTIONS

The present work is related to *SDG-12: Responsible Consumption and Production*. All the authors contributed significantly to this manuscript, participated in reviewing/editing and approved the final draft for publication. The research profile of the authors can be verified from their ORCID ids, given below:

Alphy J. Maliackal https://orcid.org/0009-0003-7366-5687
Britto S. https://orcid.org/0000-0002-3869-228X

REFERENCES

1. M.S. Rana, M. A. Rahim, M.P. Mosharraf, M.F.K. Tipu, J.A. Chowdhury, M.R. Haque, S. Kabir, M.S. Amran, and A. A. Chowdhury, *Polymers,* **15**, 1530(2023), https://doi.org/10.3390/polym15061530
2. N.H.A. Rahman, B. W. Chieng, N.A. Ibrahim, and N. Abdul Rahman, *Polymers*, **9(11)**, 588(2017), https://doi.org/10.3390/polym9110588
3. R. M. Sheltami, I. Abdullah, I. Ahmad, A. Dufresne, and H. Kargarzadeh, *Carbohydrate Polymers*, **88(2)**, 772(2012), https://doi.org/10.1016/j.carbpol.2012.01.062
4. K. Song, X. Zhu, W. Zhu, and X. Li, *Bioresources and Bioprocessing,* **6**, 45(2019), https://doi.org/10.1186/s40643-019-0279-z
5. S. C. Shi, and G. T. Liu, *Cellulose,* **28**, 6147(2021), https://doi.org/10.1007/s10570-021-03889-5
6. R. M. D. Santos, W. P. F. Neto, H.A. Silvério, D. F. Martins, N. O. Dantas, and D. Pasquini, *Industrial Crops and Products*, **50**, 707(2013), https://doi.org/10.1016/j.indcrop.2013.08.049
7. E. Hafemann, R. Battisti, D. Bresolin, C. Marangoni, and R. A. F. Machado, *Waste and Biomass Valorization,* **11**, 6595(2020), https://doi.org/10.1007/s12649-020-00937-2
8. N. T. Lam, R. Chollakup, W. Smitthipong, T. Nimchua, and P. Sukyai, *Sugar Tech* **19**, 539(2017), https://doi.org/10.1007/s12355-016-0507-1
9. M. Rasheed, M. Jawaid, B. Parveez, A. Zuriyati, and A. Khan, *International Journal of Biological Macromolecules*, **160**, 183(2020), https://doi.org/10.1016/j.ijbiomac.2020.05.170

10. I. J. C. Filho, D. P. Reis, P. H. B. Nascimento, D.S.C. Marques, and M.C.A. Lima, *Anais da Academia Brasileira de Ciências,* **95**, 20221026(2023), https://doi.org/10.1590/0001-3765202320221026
11. A. Hebeish, S. Sharaf, and M.M. Abd El-Hady, *Carbohydrate polymers*, **83(3)**, 1370(2011), https://doi.org/10.1016/j.carbpol.2010.09.052
12. L. Segal, J.J Creely, A.E. Martin, and C.M. Conrad, *Textile Research Journal*, **29(10)**,786(1959), doi:10.1177/004051755902901003
13. O. Trott, and A. J. Olson, *Journal of Computational Chemistry,* **31(2)**, 455(2010), https://doi.org/10.1002/jcc.21334
14. S.Y. Oh, D.I. Yoo, Y. Shin, and G. Seo, *Carbohydrate research*, **340(3),** 417(2005), https://doi.org/10.1016/j.carres.2004.11.027
15. H. Singh, A.K. Verma, A.K. Trivedi, and M.K. Gupta, *Materials Today: Proceedings*, **106,** 1(2024), https://doi.org/10.1016/j.matpr.2023.02.300
16. A. Mandal, and D. Chakrabarty, *Carbohydrate Polymers*, **86(3)**, 1291(2011), https://doi.org/10.1016/j.carbpol.2011.06.030
17. J.X. Sun, X.F. Sun, H. Zhao, and R.C. Sun, *Polymer Degradation and Stability*, **84(2)**, 331(2004), https://doi.org/10.1016/j.polymdegradstab.2004.02.008
18. M.H. Rubiyah, K. Melethil, S. Varghese, M. Kurian, S. Babu, L. Jojo, and B. Thomas, *Carbohydrate Polymer Technologies and Applications*, **6**, 100374(2023), https://doi.org/10.1016/j.carpta.2023.100374
19. A. Alemdar, and M. Sain, *Bioresource Technology*, **99(6)**, 1664(2008), https://doi.org/10.1016/j.biortech.2007.04.029
20. M.K. Gupta, *Journal of Industrial Textiles,* **49(7)**, 923(2018), https://doi.org/10.1177/1528083718804203
21. W. Daim, H. Uyama, and S.A. Lim, *ASEAN Journal on Science and Technology for Development*, **40(3)**, 8(2024), https://doi.org/10.61931/2224-9028.1547
22. R.K. Gond, and M.K. Gupta, *Polymer Composites*, **41(12)**, 5216(2020), https://doi.org/10.1002/pc.25788
23. N.A. Rosli, I. Ahmad, and I. Abdullah, *BioResources*, **8(2)**, 1893(2013), DOI:10.15376/biores.8.2.1893-1908
24. E.C. Sumarago, M.F.M. dela Cerna, A.K.B. Leyson, N. P. B. Tan, and K.F. Magsico, *Polymers*, **16(10),** 1312(2024), https://doi.org/10.3390/polym16101312
25. A.M. Visagamani, D. Shanthi, A. Muthukrishnaraj, B. Venkatadri, J.I. Ahamed, and K. Kaviyarasu, *ACS Omega*, **8(42),** 38860(2023), https://doi.org/10.1021/acsomega.3c02432

[RJC-9426/2025]